2019 International Conference on Robotics and Automation (ICRA)
Palais des congres de Montreal, Montreal, Canada, May 20-24, 2019

A Novel Variable Stiffness Actuator Based on Pneumatic Actuation and Supercoiled Polymer Artificial Muscles

Yang Yang, *Member, IEEE*, Zicheng Kan, Yazhan Zhang, Yu Alexander Tse, and Michael Yu Wang, *Fellow, IEEE*

***Abstract*—This article describes an innovative design of variable stiffness soft actuator, which can potentially be utilized for manipulation and locomotion of soft robots. The new actuator is a combination of two types of actuations: soft pneumatic actuation and muscle-like supercoiled polymer (SCP) actuation. Soft pneumatic actuator has two roles: first is to generate bending motions and second is to increase the stiffness of the whole actuator together with SCP artificial muscles. SCP artificial muscles are exploited to generate pre-load to resist the whole actuator from (excessive) deformation when external load is applied. These two types of actuations are arranged antagonistically to realize stiffness tuning of the whole actuator. At a given bending position, stiffness of the actuator could be tuned by controlling the pressure inside the air chamber and the tension on the SCP artificial muscles. In experimental section, tests are conducted to characterize the applied SCP artificial muscles before they are applied to the proposed actuator. Afterwards, tests of proposed actuator are performed to examine its variable stiffness capability. From experimental results, the proposed actuator can achieve 3.47 times stiffness variation ratio from 0.0312 N/mm (40 kPa air pressure and no SCP actuation) to 0.1083 N/mm (82 kPa air pressure and SCP actuation at 0.143 W/cm) at the same position (bending angle of 56 degree). This study exhibits the potential of applying SCP artificial muscles to promote the performance of soft robots.**

I. Introduction

Soft material robots have gained a lot of research interest within the last two decades owing to their advantages compared to rigid-bodied robots, including conformability to objects with various shapes, adaptability to unknown environments and safety to interact with human beings without the need for complex control loop [1-3]. Inspired by creatures from nature, soft robots have broaden the application scenarios of robots benefited from their inherent compliance.

Although lots of progress have been achieved in soft robotics field, its further application is still suffered from several considerable challenges. One of these is the ability to vary the stiffness of soft robots to fit in with the needs of different tasks [4]. Natural muscle tissues possess stiffness tunable properties to perform various tasks and to adapt to the environments. In soft robots, stiffness tunable properties are also desirable in order to transfer between rigid, load-bearing state and compliant, flexible state reversibly. To realize the variable stiffness functions of soft robot, many approaches have been proposed which can basically be divided into two groups: intrinsic adaptive material-based approach and structure-based approach [5]. Intrinsic adaptive material-based approach refers to vary stiffness using intrinsically rigidity-tunable materials [6], including shape memory polymers (SMP) [7, 8], low-melting-point alloys (LMPA) [9], jamming materials [10, 11], electrorheological fluids (ERF) [12] and magnetorheological fluids (MRF) [13], etc. Different from material-based approach, structure-based approach utilizes antagonistic arrangement of active actuation elements to realize variable stiffness [5, 14]. For example, variable stiffness can be realized by antagonistic arrangement of McKibben actuators [15], dielectric elastomer actuators (DEAs) [16], and tendons with fluidic actuators [17]. By combining soft fluidic actuators with tendon-driven actuators, researchers have designed several stiffness controllable soft manipulators that have potential applications in minimally invasive surgery (MIS) [18, 19]. In these designs, however, tendons are driven by motors, which makes the whole robotic system bulky and less cost effective. To address this problem, in this paper we have proposed a novel soft actuator by combining soft fluidic actuators with SCP artificial muscles.

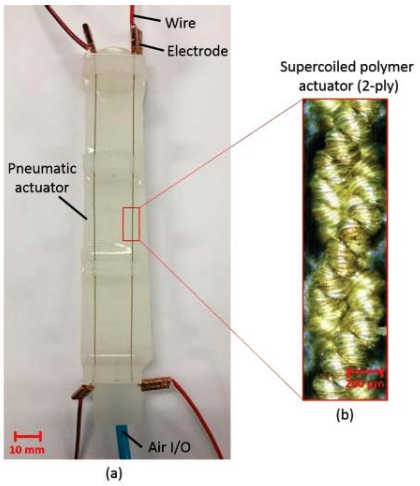

Fig. 1. Proposed novel variable stiffness soft actuator. (a) Fabricated actuator prototype. (b) Microphotograph of a 2-ply SCP actuator.

Inspired from biological muscles, artificial muscle technologies have been studied for many years such as shape memory alloy (SMA) wires [20], carbon nanotube (CNT) yarns [21] and electronic artificial muscles such as DEA [22].

*Research is supported by the Hong Kong Innovation and Technology Fund (ITF) ITS-018-17FP.

Y. Yang, Z. Kan, Y. Zhang and Y. Tse are with the Department of Mechanical and Aerospace Engineering, Hong Kong University of Science and Technology, Hong Kong (e-mail: rayang@ust.hk; zkan@connect.ust.hk; yzhangfr@connect.ust.hk; yatse@connect.ust.hk).

M. Y. Wang (corresponding author) is with the Department of Mechanical and Aerospace Engineering and the Department of Electronic and Computer Engineering, Hong Kong University of Science and Technology, Hong Kong (tel.: +852-34692544; e-mail: mywang@ust.hk).

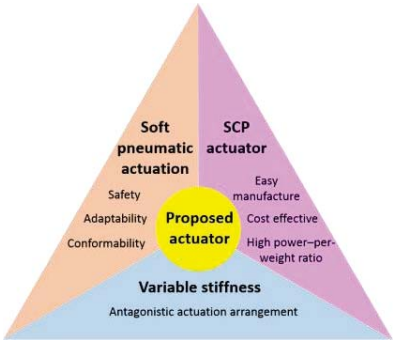

Fig. 2. Significances of proposed variable stiffness soft actuator.

Although they all have their own advantages, no technology is comparable with nature muscles considering all the following properties: power-to-weight ratio, compliance, fast action speed and high dynamic range.

Apart from these technologies, recent studies have found that a new type of artificial muscle can be obtained by twisting fishing lines and sewing threads until they are fully coiled [23]. These supercoiled polymer artificial muscles can produce tensile actuation by heating and cooling. Researchers have found that SCP artificial muscles possess attractive properties such as high power-to-weight ratio (up to 5.3 kW/kg, higher than human skeletal muscle [23]), inherent compliance, easy fabrication and low cost. Due to these superior properties, several studies of using SCP actuators in robotic applications have been reported. Yip et al. have studied the controllability and properties of SCP actuators [24]. Moreover, they applied the actuators both in a robotic arm as the bicep muscle and in a robotic hand as actuation mechanism. In their recent study, bundled SCP actuators were also developed for force amplification [25]. Wu et al. have thoroughly discussed the design of a humanoid hand actuated by SCP actuators [26]. In the study of Sutton et al., they proposed an assistive wrist orthosis driven by SCP actuators [27]. Furthermore, SCP actuators have also been applied for reconfigurable rolling robot [28] and morphing mechanism in flying robot [29]. In addition to rigid-bodied robots, SCP artificial muscles have been preliminarily studied for application in soft robots. Almubarak et al. has reported embedding SCP artificial muscles in silicone rubbers to realize undulatory and bending actuations [30]. A synthetic musculoskeletal system was developed by Wu et al. using antagonistic pairs of SCP artificial muscles for actuation [31]. In the study of Zhao et al., they also investigated a system using supercoiled conductive thread as curvature sensor for soft robot by monitoring its resistance change during motion [32]. The authors have also proposed an inchworm-inspired soft crawling robot actuated by SCP artificial muscle in recent study [33].

To the best knowledge of the authors, there is no report of SCP actuators applied for stiffness tuning of soft robots so far. Integrating SCP actuators into a soft pneumatic actuator in an antagonistic manner, a novel variable stiffness soft actuator is obtained in this study. This new actuator is motor-free, therefore eliminating complex transmission system required for electric motor and making the actuation system more compact. Moreover, the flexible SCP artificial muscles would not demerit the inherent compliance of soft actuator. The novel variable stiffness actuator is presented in Fig. 1. Fabricated

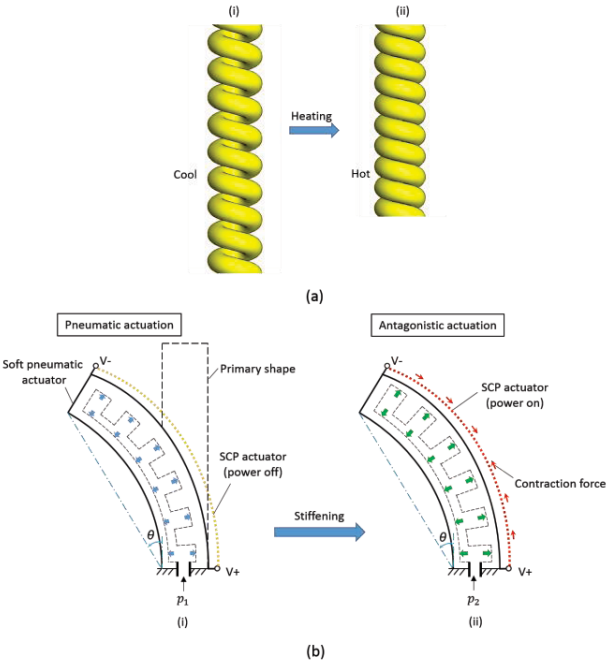

Fig. 3. Design principle of proposed actuator. (a) Contraction of the SCP actuator caused by temperature change. (i) Initial shape of SCP actuator before heating. (ii) Upon heating, axial contraction is generated along the SCP actuator. (b) Variable stiffness of the actuator by antagonistic arrangement of pneumatic actuator and SCP actuators. (i) The actuator bends to a certain position with inlet pressure p_1 of pneumatic actuator and SCP actuators powered off. (ii) The actuator increases its stiffness at the same bending position with antagonistic actuation of pneumatic actuator (inlet pressure increases to p_2) and SCP actuators (powered on).

actuator prototype is exhibited in Fig. 1(a) and microphotograph showing the supercoiled structure of a 2-ply SCP artificial muscle used in this actuator can be seen in Fig. 1(b).

This study aims to propose a new approach to realize stiffness tuning in soft actuators with the adoption of supercoiled polymer artificial muscles. Significances of this study are concluded as following (also see Fig. 2):

1. First study to apply SCP actuator for stiffness tuning of soft robots;
2. Novel design of variable stiffness actuator with antagonistic arrangement of pneumatic actuator and SCP actuator;
3. Potential application in soft manipulators and locomotion robots with variable stiffness functions.

The rest of this paper is organized as follows: Section II presents the working principle of proposed actuator, proposes a simple theoretical model for analysis and demonstrates the mechanical design of the actuator. Fabrication of the actuator is illustrated in Section III. In Section IV, characterization tests of the SCP artificial muscles used in this study are conducted, followed by actuator stiffness test to validate the variable stiffness effects of proposed approach. Finally, Section V summarizes the paper and discusses future works.

II. The Actuator Design

A. Design principle

Realization of variable stiffness using antagonistic

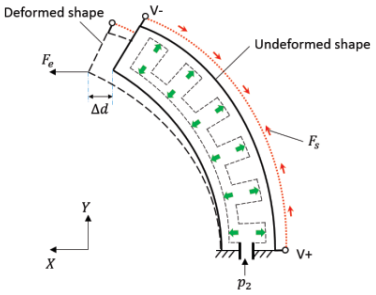

Fig. 4. Analysis of proposed variable stiffness actuator under external load.

behavior takes inspiration from creatures in nature. The octopus uses muscular antagonism of its longitudinal and transverse muscle fibers to vary the stiffness of its arm in order to perform different undersea tasks [34]. In this study, we adopt soft pneumatic actuation and SCP actuation to realize antagonism in proposed actuator. Soft pneumatic actuation provides natural and smooth motion to the actuator, enabling it with large motion range. While conductive thread SCP produces actuation strain up to 10% [24], it is not intended to provide actuation motion. Instead, SCP actuators are applied to act antagonistically with pneumatic actuator and facilitate stiffness tuning when needed. The working principle of SCP actuator is illustrated in Fig. 3(a). Upon heating, the nylon fiber will expand in its radial direction while contract in its axial direction. The supercoiled structure amplifies this thermal expansion property and as a result, notable contractions are obtained with temperature rise.

Principle of the proposed actuator's variable stiffness is illustrated in Fig. 3(b). The actuator is designed to generate bending motion while SCP actuators are arranged antagonistically with pneumatic actuation. The whole actuator bends to angle θ at inlet pressure p_1 inside air chamber of pneumatic actuator when SCP actuators are powered off (see Fig. 3(b)(i)). By activating SCP actuators and increasing air pressure to p_2 ($p_2 > p_1$) simultaneously, the actuator still holds the bending angle θ while these two types of actuations form antagonism and pre-load is generated inside the SCP actuator (see Fig. 3(b)(ii)). When external load F is applied, the deformation of the pneumatic chamber has to overcome the pre-load produced by SCP actuators. As such, stiffness of the actuator increases. By controlling the magnitude of power input of SCP actuators and inlet air pressure inside the air chamber, the proposed actuator can achieve different levels of stiffness.

B. *Analysis*

In order to describe the variable stiffness function of proposed actuator more clearly, a simple model is derived for analysis. Stiffness of a structure is defined as the ability to remain its own shape upon the application of external load. In this study, actuator stiffness k is calculated as the slope of force-displacement curve:

$$k = \frac{F_e}{d} \quad (1)$$

where F_e is the applied external force at the free end of the actuator and d is the corresponding displacement caused by the applied force.

In Fig. 4, deformation of proposed actuator under the application of external load is presented. The primary shape

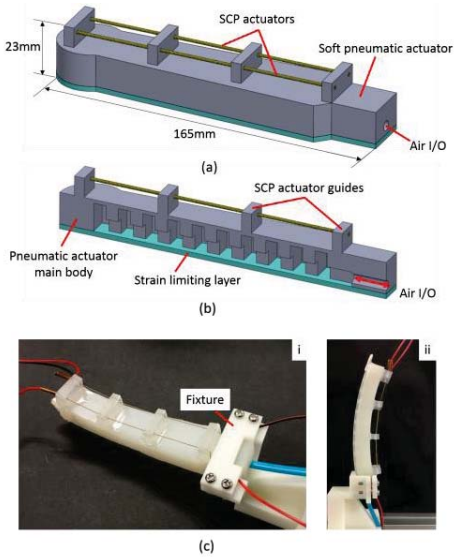

Fig. 5. Actuator mechanical design. (a) Components of proposed actuator. (b) Cross-section view showing the internal structure of the actuator. (c) Real prototype of the actuator after assembly. (i) Top view. (ii) Side view.

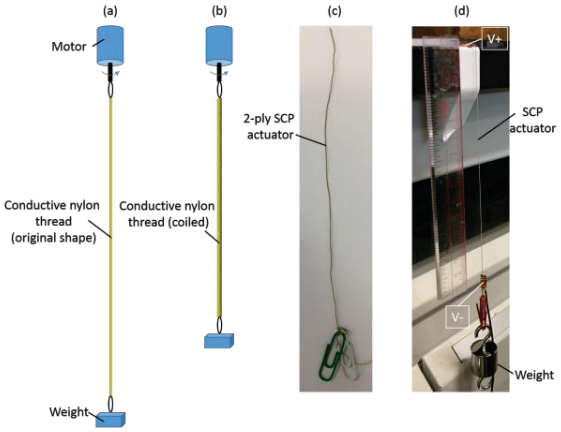

Fig. 6. Fabrication process of the SCP actuator. (a) Conductive nylon thread is attached to a motor with the other end hung by a dead weight. (b) The motor rotates and twists the nylon thread. At a certain point, coils appear along the thread. (c) After being fully coiled, the thread is double backed to form a 2-ply configuration. (d) Annealing and training of SCP actuator.

is the same as that in Fig. 3(b)(ii). After external load F_e is applied, the actuator deforms to a new position with corresponding displacement d as shown in Fig. 4. From the law of energy conservation, the work done by external load should be equal to work consumed by pneumatic actuator plus work consumed by SCP actuators, which is expressed as:

$$W_e = W_p + W_s \quad (2)$$

where W_e is the work done by external load F_e, W_p is the work consumed by pneumatic actuator and W_s is the work done by the contraction force F_s generated within SCP actuator. W_p is composed of two proportions: strain energy W_p' stored in the silicone rubber caused by deformation and W_p'' which is the work done by pressurized air.

For an element displacement Δd (within which F_e is considered as constant), SCP actuator has length variation Δl. Eq. (2) can be rewritten as:

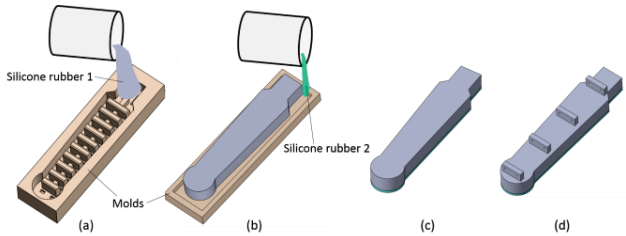

Fig. 7. Fabrication process of the pneumatic actuator. (a) 1st molding to create the main body of soft pneumatic actuator. (b) 2nd molding to create the strain limiting layer of soft pneumatic actuator. (c) Pneumatic actuator after trim of strain limiting layer from 2nd molding. (d) Fabricated pneumatic actuator with guides attached for SCP actuators.

$$F_e \Delta d = W_p + F_s \Delta l \quad (3)$$

Combining Eqs. (1) and (3), actuator stiffness k within Δd is calculated as:

$$k = \frac{F_e}{\Delta d} = \frac{W_p + F_s \Delta l}{\Delta d^2} = \frac{W_p{}' + W_p{}'' + F_s \Delta l}{\Delta d^2} \quad (4)$$

At the same bending position as shown in Fig. 3(b) and same amount of displacement Δd, $W_p{}'$ is considered to have a fixed value at different antagonistic actuation conditions. Therefore, stiffness k is increased by increasing $W_p{}''$ and F_s at a given Δd from Eq. (4). That is, stiffening can be realized by increasing inlet air pressure of pneumatic actuator and contraction force of SCP actuator, which is consistent with the design principle given in Section II-A. It is expected that larger stiffness can be achieved at larger air pressure and larger SCP actuator force output. The design principle will be validated in experimental section.

C. Actuator prototype

Based upon design principle, mechanical design of the actuator is presented in Fig. 5. The proposed actuator has two main components: a soft pneumatic actuator and a pair of SCP actuators (see Fig. 5(a)). The pneumatic actuator has four attached small guides for assembly of SCP actuators. Cross-section view (see Fig. 5(b)) shows the internal structure of the actuator. Strain limiting layer of the pneumatic actuator and the air chamber structure enable it to realize bending actuation. Real prototype of the actuator is shown in Fig. 5(c).

III. Fabrication

The fabrication of proposed actuator includes fabrication of the SCP actuator and of the pneumatic actuator separately, which will be illustrated in the following. Once fabrication of these two components are completed, the proposed actuator shown in Fig. 5 can be obtained after assembly.

A. Fabrication of the SCP actuator

The SCP actuator is formed by a conductive nylon thread (Silver Plated Nylon 66, Shieldex Conductive Yarn, 110/34 dtex HC). The silver coating enables the heating and activation of SCP actuator when directly powered on. Cost of this conductive nylon thread is around $0.03 per meter, which is much cheaper than other artificial muscles and validates the significance of being cost effective shown in Fig. 2. Fabrication process of the SCP actuator includes the following steps (see Fig. 6):

1. A conductive nylon thread is twisted until it is fully coiled; one end of the nylon thread is fixed to motor, the other end is hung by a dead weight (30g in this study) to keep the fiber straight and taut during coiling;
2. Coiled 1-ply SCP actuator is double backed to form a 2-ply actuator, which also prevents the actuator from unwinding;
3. "8"-shape compression copper sleeves are added to the ends of SCP actuator to act as electrodes for reliable connection with power supply;
4. Annealing and training of SCP actuator eliminate residual stress and large actuation capacity can be achieved.

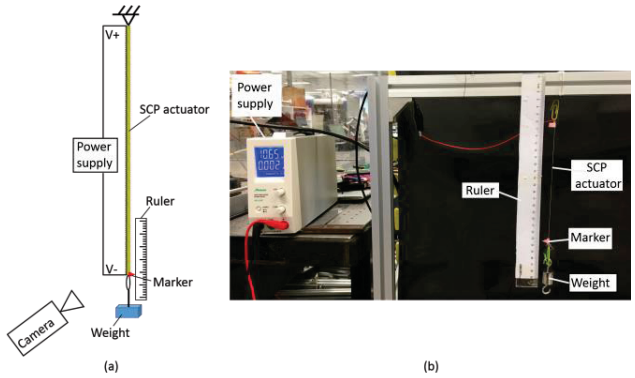

Fig. 8. Actuation stroke test. (a) Set-up diagram. (b) Real set-up.

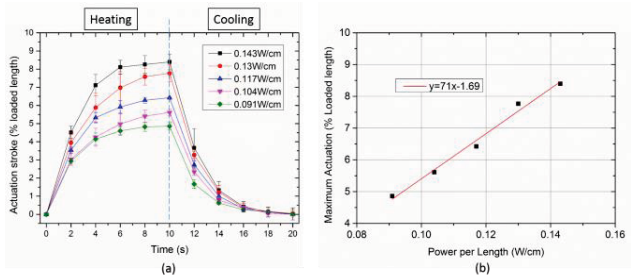

Fig. 9. Actuation stroke test results. (a) Actuation stroke (% loaded length) vs. time curve under different power per length conditions. (b) Relationship between maximum actuation stroke and power per length.

In this study, 2-ply SCP actuators are fabricated and applied in proposed actuator due to their ease of fabrication. 3-ply SCP actuators also can be fabricated by plying three 1-ply SCP actuators, which is not shown in this paper. Basically, fabrication of the SCP actuator used in this study follows the instructions from [24]. More details and precautions about the fabrication process can be found in [23], [35] and [36].

B. Fabrication of the proposed variable stiffness actuator

In this study, we expect to realize easy fabrication of the actuator. Therefore, a soft pneumatic actuator is designed that could be fabricated in a simple and fast way. Fabrication process of the pneumatic actuator is illustrated in Fig. 7, which mainly includes two-step molding. In the first step, main body of the pneumatic actuator is molded with silicone rubber 1 to obtain the air chamber (see Fig. 7(a)). In the second step, strain limiting layer is molded using silicone rubber 2 that has higher strength than silicone rubber 1 (see Fig. 7(b)). Parameters of these two types of silicone rubbers are given in Table I. All the molds are 3D printed by a commercial fused deposition modelling (FDM) 3D printer using polylactic acid (PLA) filament. After molding, guides for SCP actuators (molded in advance using silicone rubber

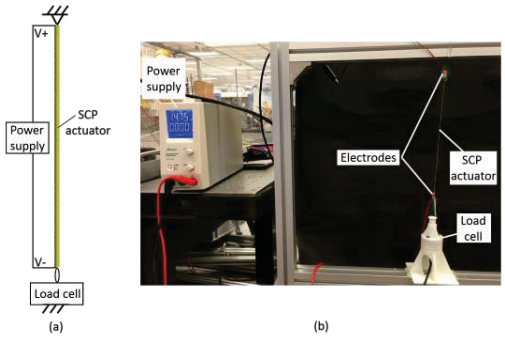

Fig. 10. Output force test set-up. (a) Set-up diagram. (b) Real set-up.

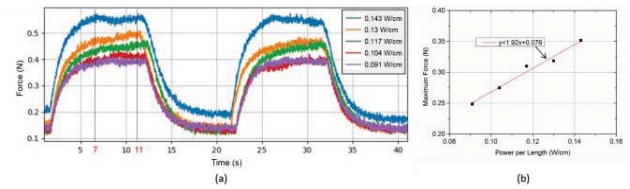

Fig. 11. Output force test results. (a) Force-time curve for two cycles under different power per length conditions. (b) Relationship between maximum output force and power per length.

2) are attached to the pneumatic actuator and the pneumatic actuator is obtained (see Fig. 7(d)). Afterwards, two SCP actuators are assembled to the pneumatic actuator body through holes in guides with pre-tension of 0.1 N. The effect of different pre-tension values on the actuator performance will be further studied in future research. The initial shape of the actuator after assembly is shown in Fig. 5(c)(ii). The curved shape from side view results from the pre-tension during assembly.

TABLE I. MAIN PARAMETERS OF SILICONE RUBBERS COMPOSING THE PNEUMATIC ACTUATOR

Properties	Silicone rubber 1 Ecoflex™ 00-50	Silicone rubber 2 Shin-Etsu RTV (KE-1310ST)
Density (g·cm^{-3})	1.07	1.08
Tensile strength (MPa)	2.17	5.7
Elongation at break (%)	320	980

IV. EXPERIMENTS AND RESULTS

In this section, firstly experiments are performed to characterize the SCP actuators fabricated in Section III-A before they are applied to the proposed variable stiffness actuator. The characterization tests include actuation stroke test and force generation test. Afterwards, we conduct stiffness test on the proposed actuator to investigate its variable stiffness function and to validate our design proposal.

A. Characterization of 2-ply SCP actuator

1) Actuation stroke test

In this test, tensile contractions of fabricated 2-ply SCP actuator are investigated upon heating with different magnitudes of power. In order to make the test result versatile to SCP actuators with different length, the power input is normalized by SCP actuator's length so that power per length is chosen as the power input unit. For consistency, the power per length in this study always refers to the electrical power applied to SCP actuator normalized by its original unloaded length. The test set-up is presented in Fig. 8. The SCP actuator

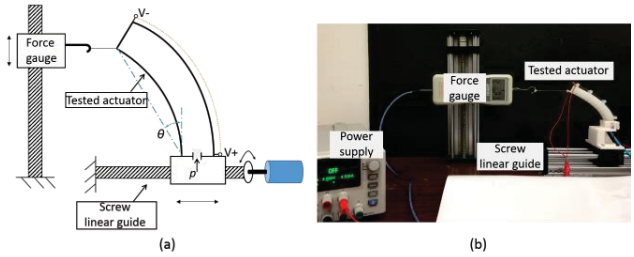

Fig. 12. Experimental set-up for stiffness test. (a) Set-up diagram. (b) Real set-up.

is fixed at one end and hung by a weight at the other end. A weight of 50 g is chosen which is the appropriate load required to act antagonistically with pneumatic actuator (actuation pressure: 0~100 kPa). The initial length of SCP actuator is 15 cm and length after loading is 16.4 cm. Actuation stroke is calculated as the ratio of contraction length to primary loaded length. A camera records the position change of marker attached to the end of the SCP actuator and thus actuation stroke is measured. The input power is provided by a DC power supply (NSP-2050, Manson Engineering Industrial Ltd.). Power per length for the SCP actuator varies from 0.091 W/cm to 0.143 W/cm with an interval of 0.013 W/cm. At 0.091 W/cm, the electrical resistance of SCP actuator is 59.2Ω. In this test, the power supply is 10 s ON for heating and 10 s OFF for cooling as a cycle. The actuation stroke is measured every 2 s. At each magnitude of power, three heating and cooling cycles are conducted. Average values as well as standard deviations are calculated and the test results are shown in Fig. 9.

In Fig. 9(a), curves of actuation stroke vs. time at different power magnitude levels are presented. It shows that 90% of both contraction (heating) and relaxation (cooling) of the SCP actuators are obtained within 6 s starting from power switch (time starts from 0 s and 10 s respectively). This offers us a reference for controlling SCP actuators in following application. In fact, faster response can be achieved by improved power input strategy such as short pulse and active cooling designs [24, 26]. As the result indicates, a maximal actuation stroke of 8.39% can be achieved at 0.143 W/cm. Besides, the actuation stroke gets larger with increase of power magnitude. To examine the relationship between maximal actuation stroke and power magnitude, Fig. 9(b) is drawn which shows a positive linear correlation between them.

2) Output force test

To investigate force generation capability, output force characterization of the same SCP actuator is performed and the experimental set-up is demonstrated in Fig. 10. One end of the SCP actuator is fixed while the other end is connected to a load cell with pre-load. In this test, the output force using a load cell (ATI mini27 Sensor) is explicitly measured. Similar to actuation stroke test, power supply is also 10 s ON and 10 s OFF but with 1~2 s delay for stable data collection. Two cycles are conducted and output force-time curve is shown in Fig. 11(a). The tendency of force variation with time is consistent with actuation stroke test. To quantify the relationship between maximum output force and power input, the average force data between 7 s to 11 s has been calculated and then the initial force shown in Fig. 11(a) is deducted to get the maximal output

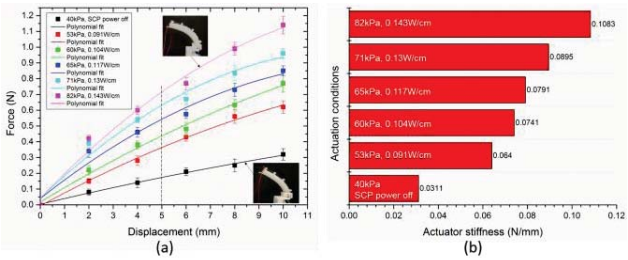

Fig. 13. Actuator stiffness test results. (a) Force-displacement curve at different antagonistic actuation conditions. (b) Actuator stiffness (experimental values obtained from force-displacement curve) at different antagonistic actuation conditions.

force for each power magnitude and the results are illustrated in Fig. 11(b). It is obvious that the output force also gets larger with increase of power magnitude. The output force achieves 0.25 N at 0.091 W/cm and 0.35 N at 0.143 W/cm. The data in Fig. 11(b) is also positively correlated.

B. Characterization of proposed variable stiffness actuator

Based on the design principle and analysis, it is expected that stiffness of proposed variable stiffness actuator can be tuned by varying the power magnitude of SCP actuators and the input air pressure of the pneumatic actuator simultaneously. With characterization results of SCP actuators obtained, test on the assembled actuator can be operated. In this section, actuator stiffness test is performed to verify our design proposal.

Based upon the stiffness definition given in Section II-B, experimental set-up of the stiffness test is presented in Fig. 12. The tested actuator is mounted on a motor-driven screw linear guide. A digital force gauge (range: 0–10 N, precision: 0.01 N) is used to measure the applied force F on the actuator when the tested actuator moves horizontally on the linear guide. The displacement d at the actuator end is controlled to range within 0~10 mm with an interval of 2 mm. At each displacement, the force gauge records the corresponding applied force.

In this test, the tested actuator is actuated to form a bending angle θ=56° for case study. Bending angle θ is measured using a coordinate paper. Power input for both SCP actuators varies from 0.091 W/cm to 0.143 W/cm, same as the characterization test. Inlet air pressure of the pneumatic actuator is regulated by pressure control valve (SMC ITV1030-212L, output 0.005~0.5MPa). The test is conducted at different antagonistic actuation conditions. The first condition is pneumatic actuation only at 40 kPa with SCP actuators powered off, followed by 53 kPa, 0.091 W/cm; 60 kPa, 0.104 W/cm; 65 kPa, 0.117 W/cm; 71 kPa, 0.13 W/cm and 82 kPa, 0.143 W/cm, in total 6 antagonistic actuation conditions. At each condition, the measurement is repeated three times and average values are calculated. The force-displacement data obtained is presented in Fig. 13(a). Since the data seem to have non-linear variation trend, polynomial fitting (two order) is performed. The force-displacement fitting curves are approximately linear when displacement falls within the range of 0~5 mm. At displacement Δd=5mm (Δd is small compared to the total length of the actuator), slopes of the curves are calculated as experimental stiffness values.

From force-displacement curve, applied force on the actuator is larger as input pressure and power magnitude increase at the same displacement. At displacement of 10 mm, applied force is 1.14 N for 82 kPa, 0.143 W/cm and only 0.62 N for 53 kPa, 0.091 W/cm. The applied force with no SCP actuation and air pressure 40 kPa is even smaller, as 0.32 N. From experimental stiffness values in Fig. 13(b), stiffness variation ratio of the proposed actuator can achieve 3.48 times from 0.1083 N/mm (82 kPa, 0.143 W/cm) to 0.0311 N/mm (40 kPa, no SCP actuation) at the same bending angle. Furthermore, the ratio is 1.69 from 0.1083 N/mm (82 kPa, 0.143 W/cm) to 0.064 N/mm (53 kPa, 0.091 W/cm). The experimental result validates our design proposal of realizing variable stiffness at the same position by antagonistic arrangement of SCP actuator and pneumatic actuator.

V. CONCLUSION AND DISCUSSION

In this article, we have developed an innovative variable stiffness soft actuator by combining soft pneumatic actuation with SCP artificial muscles. The actuation arrangement of these two actuation elements is able to vary the stiffness of proposed actuator by generating preload to resist deformation caused by external load. We have fabricated an actuator prototype based upon the design principle and performed experiments to validate its variable stiffness function. Through experiments, the actuator can achieve stiffness tuning by adopting the antagonistic actuation principle. This study shows the potential of applying SCP artificial muscles in soft robots not only for actuation but also for variable stiffness functions. We believe that SCP artificial muscles can open up more possibilities in soft robotics field due to their superior properties.

It is worth mentioning that the proposed actuator is also perceptive which is another essential function expected in soft robots [37]. The resistance of conductive supercoiled nylon thread is found to change linearly with respect to its elongation due to the variation in cross section area [32]. In our design, SCP artificial muscles can act as curvature sensors when they are powered off (Fig. 3(b)(i)) by monitoring their resistance change during motion. This endows the actuator with multifunction: not only variable stiffness but also curvature sensing. Sensor calibration and curvature feedback evaluation will be conducted in future works.

The application of SCP artificial muscles in realizing the stiffness tuning of soft actuator still has some challenges to overcome such as actuation speed and initial pre-stress in assembly that need to be further investigated in order to improve its performance. In future research, we hope to develop actuators with more pneumatic chambers and different SCP artificial muscles configuration for stiffness tuning at more directions. Performance of SCP artificial muscles will also be improved. For example, bundled SCP artificial muscles can offer larger output force and could be applied to realize a larger ratio of stiffness variation. Moreover, thermal sensor could be added to the SCP artificial muscles for close loop control [24, 38]. We also intend to apply the actuators in real application scenarios, such as soft grippers, soft locomotion robot and soft wearable devices.

REFERENCES

[1] C. Majidi, "Soft robotics: a perspective—current trends and prospects for the future," *Soft Robot.,* vol. 1, no. 1, pp. 5-11, 2014.

[2] G. M. Whitesides, "Soft robotics," *Angew. Chem. Int. Ed.*, vol. 57, no. 16, pp. 4258-4273, 2018.

[3] J. Shintake, V. Cacucciolo, D. Floreano, and H. Shea, "Soft Robotic Grippers," *Adv. Mater.,* vol. 30, no. 29, p.1707035, 2018.

[4] C. Laschi, B. Mazzolai, and M. Cianchetti, "Soft robotics: Technologies and systems pushing the boundaries of robot abilities," *Sci. Robot.,* vol. 1, no. 1, eaah3690, 2016.

[5] M. Manti, V. Cacucciolo, and M. Cianchetti, "Stiffening in soft robotics: a review of the state of the art," *IEEE Robot. Autom. Mag.*, vol. 23, no. 3, pp. 93-106, 2016.

[6] L. Wang, Y. Yang, Y. Chen, C. Majidi, F. Iida, E. Askounis, and Q. Pei, "Controllable and reversible tuning of material rigidity for robot applications," *Mater. Today*, vol. 21, no. 5, pp. 563-576, 2018.

[7] Y. Yang, Y. Chen, Y. Li, M. Z. Chen, and Y. Wei, "Bioinspired robotic fingers based on pneumatic actuator and 3D printing of smart material," *Soft Robot.,* vol. 4, no. 2, pp. 147-162, 2017.

[8] Y. Yang, Y. Chen, Y. Li, Z. Wang, and Y. Li, "Novel variable-stiffness robotic fingers with built-in position feedback," *Soft Robot.*, vol. 4, no. 4, pp.338-352, 2017.

[9] Y. Hao, T. Wang, Z. Xie, W. Sun, Z. Liu, X. Fang, M. Yang, and L. Wen, "A eutectic-alloy-infused soft actuator with sensing, tunable degrees of freedom, and stiffness properties," *J. Micromech. Microeng.*, vol. 28, no. 2, p.024004, 2018.

[10] E. Brown, N. Rodenberg, J. Amend, A. Mozeika, E. Steltz, M.R. Zakin, H. Lipson, and H.M. Jaeger, "Universal robotic gripper based on the jamming of granular material," *Proc. Nat. Acad. Sci.,* vol. 107, no. 44, pp. 18809-18814, 2010.

[11] Y. Li, Y. Chen, Y. Yang, and Y. Wei, "Passive particle jamming and its stiffening of soft robotic grippers," *IEEE Trans. Robot.,* vol. 33, no. 2, pp.446-455, 2017.

[12] A. Sadeghi, L. Beccai, and B. Mazzolai, "Innovative soft robots based on electro-rheological fluids," in *Proc. IEEE/RSJ Int. Conf. Intell. Robot. Syst.,* 2012, pp. 4237-4242.

[13] A. Pettersson, S. Davis, J.O. Gray, T.J. Dodd, and T. Ohlsson, "Design of a magnetorheological robot gripper for handling of delicate food products with varying shapes," *J. Food Eng.,* vol. 98, no. 3, pp.332-338, 2010.

[14] Y. Yang, Y. Li, and Y. Chen, "Principles and methods for stiffness modulation in soft robot design and development," *Bio-Design and Manufacturing*, vol. 1, no. 1, pp. 14-25, 2018.

[15] K. Suzumori, S. Wakimoto, K. Miyoshi, and K. Iwata, "Long bending rubber mechanism combined contracting and extending fluidic actuators," in *Proc. IEEE/RSJ Int. Conf. Intell. Robot. Syst.,* 2013, pp. 4454-4459.

[16] R. Pelrine, et al., "Variable stiffness mode: devices and applications," in *Dielectric elastomers as electromechanical transducers: fundamentals, materials, devices, models and applications of an emerging electroactive polymer technology*. Oxford, Elsevier, 2008, pp. 141–145.

[17] A. Stilli, H.A. Wurdemann, and K. Althoefer, "Shrinkable, stiffness-controllable soft manipulator based on a bio-inspired antagonistic actuation principle," in *Proc. IEEE/RSJ Int. Conf. Intell. Robot. Syst.,* 2014, pp. 2476-2481.

[18] F. Maghooa, A. Stilli, Y. Noh, K. Althoefer, and H.A. Wurdemann, "Tendon and pressure actuation for a bio-inspired manipulator based on an antagonistic principle," in *Proc. IEEE Int. Conf. Robot. Autom.,* 2015, pp. 2556-2561.

[19] A. Shiva, A. Stilli, Y. Noh, A. Faragasso, I. De Falco, G. Gerboni, M. Cianchetti, A. Menciassi, K. Althoefer, and H.A. Wurdemann, "Tendon-based stiffening for a pneumatically actuated soft manipulator," *IEEE Robot. Autom. Lett.,* vol. 1, no. 2, pp.632-637, 2016.

[20] J. D. Madden et al., "Artificial muscle technology: physical principles and naval prospects," *IEEE J. Ocean. Eng.,* vol. 29, no. 3, pp.706-728, 2004.

[21] M. D. Lima et al., "Electrically, chemically, and photonically powered torsional and tensile actuation of hybrid carbon nanotube yarn muscles," *Science*, vol. 338, no. 6109, pp. 928–932, 2012.

[22] T. Mirfakhrai, J.D. Madden, and R.H. Baughman, "Polymer artificial muscles," *Mater. Today*, vol. 10, no. 4, pp.30-38, 2007.

[23] C. S. Haines et al., "Artificial muscles from fishing line and sewing thread," *Science*, vol. 343, no. 6173, pp. 868–872, 2014.

[24] M. C. Yip and G. Niemeyer, "On the control and properties of supercoiled polymer artificial muscles," *IEEE Trans. Robot.*, vol. 33, no. 3, pp. 689–699, 2017.

[25] A. Simeonov et al., "Bundled Super-Coiled Polymer Artificial Muscles: Design, Characterization, and Modeling," *IEEE Robot. Autom. Lett.,* vol. 3, no. 3, pp.1671-1678, 2018.

[26] L. Wu, M. J. de Andrade, L. K. Saharan, R. S. Rome, R. H. Baughman, and Y. Tadesse, "Compact and low-cost humanoid hand powered by nylon artificial muscles," *Bioinspir. Biomim.*, vol. 12, no. 2, p. 026004, 2017.

[27] L. Sutton, H. Moein, A. Rafiee, J. D. W. Madden, and C. Menon, "Design of an assistive wrist orthosis using conductive nylon actuators," in *Proc. of IEEE Inter. Conf. Biomed. Robot. Biomech.*, 2016, pp. 1074–1079.

[28] L. Wu, M. J. de Andrade, T. Brahme, Y. Tadesse, and R. H. Baughman, "A reconfigurable robot with tensegrity structure using nylon artificial muscle," in *SPIE Smart Structures and Materials+ Nondestructive Evaluation and Health Monitoring*, 2016, pp. 97993K–97993K, International Society for Optics and Photonics.

[29] H. Li, L. Liu, T. Xiao, and H. Ang, "Design and simulative experiment of an innovative trailing edge morphing mechanism driven by artificial muscles embedded in skin," *Smart Mater. Struct.*, vol. 25, no. 9, p. 095004, 2016.

[30] Y. Almubarak, and Y. Tadesse, "Twisted and coiled polymer (TCP) muscles embedded in silicone elastomer for use in soft robot," *Int. J. Intell. Robot. Appl.,* vol. 1, no. 3, pp. 352-368, 2017.

[31] L. Wu, I. Chauhan, and Y. Tadesse, "A Novel Soft Actuator for the Musculoskeletal System," *Adv. Mater. Technol.*, vol. 3, no. 5, p.1700359, 2018.

[32] J. Zhao and A. Abbas, "A low cost soft coiled sensor for soft robots," in *ASME Dynamic Systems and Control Conference (DSCC)*, 2016, p. V002T26A006.

[33] Y. Yang, Y. Tse, Y. Zhang, Z. Kan and M. Y. Wang, "A Low-cost Inchworm-inspired Soft Robot Driven by Supercoiled Polymer Artificial Muscle, " in *Proc. IEEE Int. Conf. Soft Robot.,*2019 (accepted)

[34] W.M. Kier and M.P. Stella, "The arrangement and function of octopus arm musculature and connective tissue," *J. Morphol.*, vol. 268, no. 10, pp. 831-843, 2007.

[35] J. Zhang, K. Iyer, A. Simeonov, and M. C. Yip, "Modeling and inverse compensation of hysteresis in supercoiled polymer artificial muscles," *IEEE Robot. Autom. Lett.*, vol. 2, no. 2, pp. 773–780, 2017.

[36] M. C. Yip and G. Niemeyer, "High-performance robotic muscles from conductive nylon sewing thread," in *Proc. IEEE Int. Conf. Robot. Autom.,* 2015, pp. 2313–2318.

[37] H. Wang, M. Totaro, and L. Beccai, "Toward Perceptive Soft Robots: Progress and Challenges," *Adv. Sci.*, p.1800541, 2018.

[38] T.A. Luong, K.H. Cho, M.G. Song, J.C. Koo, H.R. Choi, and H. Moon, "Nonlinear Tracking Control of a Conductive Supercoiled Polymer Actuator," *Soft Robot.,* vol. 5, no. 2, pp. 190-203, 2018.